Curvature and Size Effects Hinder Halogen Bonds with Extended π Systems

Enrique M. Cabaleiro-Lago[a] and Jesús Rodríguez-Otero[b]

[a] Departamento de Química Física, Facultade de Ciencias, Universidade de Santiago de Compostela, Campus de Lugo, Av. Alfonso X El Sabio, s/n 27002 Lugo, Galicia (Spain).
[b] Departamento de Química Física, Facultade de Química, Universidade de Santiago de Compostela, 15782 Santiago de Compostela , Galicia (Spain).

Abstract

Curvature and size effects in halogen interactions with extended aromatic species have been evaluated, employing computational methods, in dimers formed by the dihalogens Cl_2, Br_2 and I_2 with both planar (coronene and circumcoronene) and curved (corannulene, sumanene and C_{60}) aromatic systems. The main controlling factor in these interactions is dispersion, so they become stronger as the size of the halogen growths. The nature of the interaction with the halogen changes depending on the curvature and the extension of the aromatic system. As the aromatic species becomes larger, parallel stacked structures are favoured by dispersion increases over halogen bonded ones. Parallel dimers by the concave side are also favoured as the curvature of the aromatic species increases, while the effect is the opposite by the convex side. Overall, halogen bond interactions are not favoured for large planar or curved aromatic systems; only by the convex face of the most curved structures the dispersion contribution decreases enough as to make halogen bonded structures competitive with parallel stacked ones.

1. Introduction

Aromatic systems display a great versatility when it comes to establishing interactions with another species. Non covalent interactions involving π systems are a frequent and crucial motif in a variety of fields in chemistry, biology and materials science,[1-3] controlling the behaviour of extended π systems of interest such as fullerenes, carbon nanotubes and graphene flakes.[4, 5] Typically, aromatic systems participate in π-π, XH-π, or ion-π interactions.[2, 6] π-π interactions are controlled by dispersion and are usually referred to as π-π stacking. The term has been recently revised,[7] since it seems that the interactions between aromatic systems only have a certain special character when the aromatic system is extended.[8-11] The ion-π interactions between charged species and aromatic systems are among the most intense in the gas phase. The interaction between a cation and an aromatic species is normally controlled by the electrostatic contribution, although with important contributions of induction.[12, 13] In the case of anion-π interactions, the contribution of dispersion is usually larger.[14, 15] With regard to the XH-π interactions, these are similar to a hydrogen bond with the aromatic species acting as an acceptor, though in general they have a greater dispersive component. [16, 17]

In addition to these typical kinds of interactions involving aromatic systems, other interacting motifs have been identified in recent years. Among these interactions is the halogen bond or, more generally, interactions by means of a σ-hole, that have shown a great potential for multiple applications, from new anionic receptors to catalysts.[18-21] In many species, a partially positive region is generated due to a relative deficiency in electron density, normally located in a region opposing a bond.[22-26] For instance, in dihalogen molecules X_2, a region with positive Molecular Electrostatic Potential (MEP) is created, which becomes larger and more positive as the halogen size increases (maximum values of 26, 28 and 30 kcal mol^{-1} for chlorine, bromine and iodine, respectively.[22] This positive region can interact favourably with negative regions in a different molecule, leading to interactions with an important electrostatic component. Studies on the interaction between halogens and aromatic species are less frequent, but they seem to indicate that dispersion plays a major role, even surpassing electrostatics.[20, 27-31] However, the size of the aromatic system is relevant, as shown by Kim et al. in previous work on the interaction of halogens with a series of aromatic systems of increasing size.[31] The authors raise a warning about how the use of small aromatic species as models can distort the predictions made for more extended aromatics. In fact, there is a change in the orientation of the halogen when the size of the system increases; while in small systems a halogen bond is formed, in the larger ones a parallel stacked structure seems to be preferred.

An interesting aspect of the interactions with aromatic systems has arisen from the appearance of aromatic species with curved surfaces, such as fullerenes, nanotubes or buckybowls.[32-34] The curvature of the aromatic surface in these species alters the characteristics of their interactions. In a previous study,[35] Kennedy et al. have considered the effect of the curvature upon the stacking interaction in coronene and corannulene dimers. The results show that the curvature always strengthens the interaction because a permanent dipole is generated in the curved species, but also because curvature allows atoms to be closer together, increasing the contribution of dispersion. In fact, this complementarity between curved aromatic surfaces (concave-convex π-π interaction) is the main design parameter of many fullerene receptors,[5, 36] such as Sygula's tweezer,[37] buckybowls[38-44] and cycloparaphenylenes.[45-53] Also, the curvature

produces a greater dispersive component in the interaction with anions and cations by the concave face of buckybowls, so that it can even dominate over the electrostatic component in complexes with polyatomic ions.[54-57]

Considering the importance of these species with curved surfaces, it is crucial to have a deep knowledge of their interactions and how they differ from their flat analogues. This paper presents a study on the interaction of the dihalogen molecules Cl_2, Br_2 and I_2 with curved and flat extended aromatic species (see Figure 1). Complexes with the planar coronene ($C_{24}H_{12}$) are employed as a reference system to check curvature effects in the similarly-sized buckybowls corannulene ($C_{20}H_{10}$) and sumanene ($C_{21}H_{12}$). The effects of extending the aromatic surface are checked by considering complexes with the larger circumcoronene ($C_{54}H_{18}$) and fullerene C_{60}. The results will hopefully provide information on how curvature affects the interaction between halogen molecules and curved surfaces, and which are the factors determining the characteristics of this type of interactions.

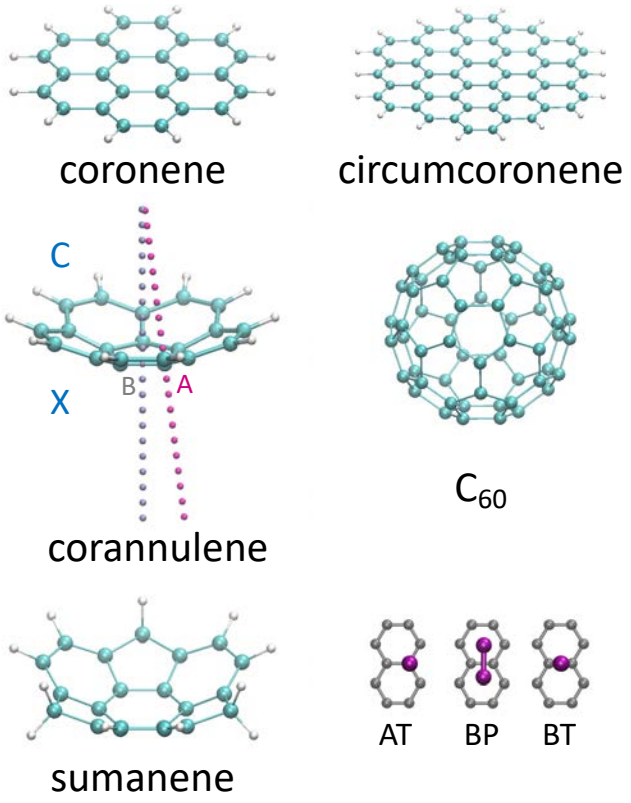

Figure 1. Aromatic species considered in this work. Corannulene also shows the lines crossing a carbon atom (A) and a C-C midbond (B) employed for the potential energy scans (see text). C and X indicate the conCave and conveX faces of curved systems. Also included (bottom, right) there is a schematic representation of the orientations employed for the dihalogen molecules.

2. Computational Details

The geometry of each of the species considered in this work has been optimised by using the TPSS functional empirically corrected to take account of dispersion with the D3BJ model by Grimme,[58-60] together with the def2-TZVP basis set.[61] In I_2-containing species the def2-ECP pseudopotential has been employed as implemented in Orca 4.1.[62] Dimers have been constructed by putting the geometrical centre of X_2 (X = Cl, Br, I) on top of a carbon atom (A) and on top of a C-C midbond (B) belonging to the innermost ring of each aromatic species (Figure 1). In the latter case two orientations have been considered, with the halogen σ-hole pointing towards the aromatic system (T) and with the halogen molecule parallel to the aromatic surface (P). With these three orientations (AT, BP and BT, see Fig. 1 and Fig. S1) potential energy scans are carried out by changing the distance between X_2 and the aromatic molecule, always keeping the geometry of the molecules frozen at the values obtained at the TPSS-D3BJ/def2-TZVP level. In the case of the planar species, the halogen is simply displaced along the *z* coordinate (the aromatic species is in the *xy* plane), but in the case of the curved systems the procedure is somewhat more involved. To perform scans in the curved species, the carbon skeleton of corannulene and sumanene has been fitted to a sphere, and the scanning directions are defined by lines going from the centre of the sphere to a carbon atom (A) or to a centre of a C-C bond (B) (See Figure 1 for a representation of the scanning directions in corannulene). Since buckybowls have two different surfaces, the scans have been performed for both the concave and convex surfaces.

For each of the dimer structures, the interaction energy has been obtained by using the supermolecule method applying the counterpoise correction to correct from basis set superposition error.[63, 64] As indicated by Kim et al.,[31] the preference for the T-shaped or parallel orientations in coronene complexes is subtle, with almost isoenergetic structures. Thus, even though in a previous study TPSS-D3BJ has shown to provide reasonable results for the interaction in buckybowl dimers,[65] the interaction energy has been obtained with several other methods for dimers formed with coronene, corannulene and sumanene; namely, B3LYP-D3BJ/def2-TZVP, SCS-MP2/CBS,[66-68] MP2.5,[69] MP2.X[70-72] and SAPT0/jun-cc-pVDZ.[73, 74]

The interaction energy has been estimated at the complete basis set limit (CBS) using the MP2 method. To this end, extrapolation of the correlation energy following the scheme proposed by Helgaker[75, 76] has been done by using the aug-cc-pVDZ and aug-cc-pVTZ basis sets. Thus, the MP2/CBS interaction energy is obtained as:

$$\Delta E_{MP2}^{CBS} = \Delta E_{HF}^{AVTZ} + \frac{X^3}{X^3-(X-1)^3}\Delta \mathrm{E}_{\mathrm{corr,MP2}}^{\mathrm{AVTZ}} - \frac{(X-1)^3}{X^3-(X-1)^3}\Delta \mathrm{E}_{\mathrm{corr,MP2}}^{\mathrm{AVDZ}};\ \mathrm{X}{=}3 \quad \text{(eq. 1)}$$

However, MP2 tends to overestimate the interaction energy in this kind of systems, so a higher-order correction must be included. A cheap way to do this is by scaling the contributions from equal and different spin electron pairs in the so-called SCS-MP2 method proposed by Grimme.[66-68] In this method, the contributions to the correlation energy from electron pairs with the same spin are scaled by 1/3, while those with antiparallel spin are scaled by 6/5. The SCS-MP2/CBS interaction energy has been obtained by using an expression like equation 1 with the proper scaling factors.

In the MP2.5 method,[69, 70] a higher order correction obtained at the MP3/aug-cc-pVDZ level is added to the MP2/CBS interaction energies. Thus:

$$\Delta E_{MP2.5} = \Delta\, E_{MP2}^{CBS} + 0.50\ (\Delta \mathrm{E}_{\mathrm{corr,MP3}}^{\mathrm{AVDZ}} - \Delta \mathrm{E}_{\mathrm{corr,MP2}}^{\mathrm{AVDZ}}) \qquad \text{(eq. 2)}$$

and the correction is simply half the contribution of the third order energy to the interaction energy. The cheaper MP2.X approach is similar but using a smaller basis set for the MP3 calculation and a scaling parameter (0.72 instead of 0.50 in eq. 2 with the cc-pVDZ basis set).[72]

The interaction energies have also been obtained applying Symmetry Adapted Perturbation Theory (SAPT) methods.[77-79] SAPT methods not only provide the interaction energy but also its different components. Thus, the SAPT interaction energy is obtained as a sum of contributions that can be identified with electrostatic, induction, exchange-repulsion and dispersion contributions. Considering the size of the systems studied, the simplest SAPT level, SAPT0,[74, 78] will be applied, including the following terms:

$$E_{SAPT0} = E_{electr}^{10} + E_{exch}^{10} + E_{ind}^{20} + E_{exch,ind}^{20} + E_{disp}^{20} + E_{exch,disp}^{20} + \delta HF$$

with δHF being a term trying to represent induction to higher orders. The contributions are usually grouped as follows: $E_{ele}=E^{10}_{electr}$; $E_{rep}=E^{10}_{exch}$; $E_{ind}=E^{20}_{exch,ind} + E^{20}_{ind} + \delta HF$; $E_{dis}=E^{20}_{exch,dis} + E^{20}_{dis}$, corresponding to electrostatic, repulsion, induction and dispersion contributions to the interaction. In this work, the SAPT0 method will be applied together with the jun-cc-pVDZ basis set, which has been shown to provide appropriate results for a variety of complexes at a moderate computational cost.[74]

DFT and MP3 calculations have been performed with Orca 4.1[62] by using the resolution of the identity approach (Weigend def2/J[79] auxiliary basis set) and the chain of spheres approach (RIJCOSX)[80, 81] in B3LYP and MP3. MP2 and SAPT calculations have been carried out with Psi4 v1.3.2.[82] For iodine, the pseudopotential (aug-cc-pVXZ), orbital (aug-cc-pVXZ) and jkfit basis sets (def2-universal JKFIT) have been taken from the EMSL,[83, 84] while auxiliary basis sets for MP2 were obtained from Hättig.[85]

3. Results

3.1. Complexes with coronene, corannulene and sumanene

3.1.1. Performance of the different methods employed

The whole set of potential energy curves is listed in Supporting Information (Figs. S2 to S7; Tables 1 and S1 to S6 for values at the minima of the curves). Taking the MP2.5 results as a reference, all the methods perform fairly well, though showing deviations that in several cases are significant. The best behaviour is obtained with SCS-MP2/CBS, which closely reproduces the values obtained at the MP2.5 level avoiding the costly MP3 calculation. The deviations barely reach 0.1 kcal mol^{-1}, and the equilibrium distances are also well reproduced. Both DFT methods roughly reproduce the MP2.5 values, but it can be observed that TPSS-D3BJ shows some problems for complexes with the convex side of corannulene and sumanene, leading to somewhat too short equilibrium distances. B3LYP-D3BJ offers a better description of the

interaction energies, but in turn shows deviations for complexes by the concave side of the buckybowls, leading to too large equilibrium distances. Quite surprisingly, SAPT0 gives a very good estimation of the equilibrium distances in all complexes. Also, the interaction energies are pretty good, with a performance better than TPSS and just slightly worse than B3LYP (mostly in I_2 complexes). MP2.X behaves worse than SCS-MP2/CBS despite needing extra MP3/cc-pVDZ calculations, so it offers no advantage for studying larger systems. Therefore, to study larger complexes the best approach could be to obtain the equilibrium geometries with SAPT0, and then to refine the interaction energies at the SCS-MP2/CBS level, if necessary.

3.1.2. Characteristics of the complexes at the MP2.5 level

Once the scans are performed for the different complexes, the equilibrium geometry for each orientation is obtained by interpolation of the potential energy curves. The results are summarised in Table 1 for the 45 dimers considered. In the case of corannulene and sumanene there are two possibilities depending on whether the interaction takes places by the concave or the convex side of the bowl, which will be denoted as C and X respectively in the following (see also Figure 1).

Table 1. Equilibrium distance R (Å, to the centre of the X_2 bond) and interaction energy E (kcal mol^{-1}) for the complexes of Cl_2, Br_2 and I_2 with coronene (**coro**), corannulene (**cora**), and sumanene (**suma**) as obtained by interpolation of the MP2.5 potential energy curves. C and X refer to the concave and convex sides of the bowls, respectively.

		AT		BP		BT	
		R	**E**	**R**	**E**	**R**	**E**
Cl_2	**coro**	4.03	-4.57	3.35	-4.80	4.05	-4.45
	cora-X	3.95	-3.84	3.29	-3.41	4.02	-3.65
	cora-C	4.20	-5.98	3.61	-6.66	4.15	-6.04
	suma-X	3.96	-3.74	3.30	-3.23	3.98	-3.91
	suma-C	4.23	-6.42	3.71	-6.46	4.19	-6.45
Br_2	**coro**	4.21	-5.97	3.46	-5.83	4.24	-5.80
	cora-X	4.10	-5.26	3.38	-4.22	4.18	-4.93
	cora-C	4.43	-7.43	3.76	-7.80	4.38	-7.51
	suma-X	4.11	-5.13	3.37	-4.05	4.12	-5.40
	suma-C	4.46	-7.96	3.89	-7.46	4.42	-8.00
I_2	**coro**	4.53	-7.38	3.63	-7.09	4.55	-7.22
	cora-X	4.40	-6.48	3.50	-5.26	4.49	-6.11
	cora-C	4.77	-9.12	4.02	-8.64	4.72	-9.21
	suma-X	4.41	-6.32	3.46	-5.16	4.42	-6.60
	suma-C	4.80	-9.77	4.17	-8.08	4.76	-9.83

The dihalogens considered show a σ-hole on the molecular axis displaying a positive Molecular Electrostatic Potential (MEP). The maximum value for the MEP on an isodensity surface of 0.001 a.u. at the TPSS-D3BJ/def2-TZVP level amounts to 26 kcal mol^{-1}, 30 kcal mol^{-1} and 32 kcal mol^{-1} for Cl_2, Br_2 and I_2, respectively, in agreement with published data (see Fig. S8).[22] As expected, the size and magnitude of the σ-hole increases with the size of the halogen. Thus, if the σ-hole is oriented toward the π surface (AT or BT orientations), it is expected that the complex will be more stabilised by electrostatic interactions as the size of the halogen grows. This larger interaction is in competition with an increment in dispersion as the halogen grows, which is maximised if the halogens are parallel and therefore closer to the π surface (BP).

The results indicate that the interaction strengthens as the halogen size increases, both in P and T orientations. For instance, complexes of Cl_2 with coronene show interaction energies around -4.5 to -4.8 kcal mol^{-1}, slightly favouring the BP structure. In Br_2 complexes, though, the interaction increases to around -5.8 to -6.0 kcal mol^{-1}, being AT slightly favoured. The trend is confirmed in I_2 complexes, with interaction energies around -7.1 to -7.4 kcal mol^{-1}, also favouring AT structures. Therefore, the increase in the value of the σ-hole somehow outweighs the possible increase in dispersion in BP structures (in any case, energy differences are small and barely reach 0.3 kcal mol^{-1} among the different orientations).

The behaviour can be more clearly seen in Figure 2, showing the energy profiles of complexes with corannulene (coronene and sumanene in Fig. S9). It can be observed that, as the halogen increases its size, the complexes formed become more stable while the equilibrium distance also increases. In the case of the complexes by the convex face (Figure 2, left) the trends are similar to those observed in coronene, though the AT complex is the most stable one in the three complexes with corannulene, while BT is the most favoured orientation in sumanene complexes. The situation is different by the concave side; corannulene BP complexes with Cl_2 and Br_2 are the most stable ones because by this face there is an increase associated to dispersion since the carbon atoms surround and somewhat encapsulate the X_2 molecule. Due to its larger size I_2 does not fit well into corannulene, so the most stable minimum is BT. Sumanene complexes behave similarly, but BT is favoured, except in the case of Cl_2. It is worth noting that by the concave face the distinction between AT, BT and BP somewhat fades, because X_2 can also interact with other regions of the bowl far from the atoms employed for defining the scan directions.

Considering the complexes with Cl_2 as a reference, it can be observed (Table 1 and Figure 2) that by the convex side the presence of Br_2 implies an increase in the interaction of -1.4 to -1.5 kcal mol^{-1}, while changing to I_2 the increment is between -2.5 and -2.8 kcal mol^{-1}. Changes are similar, or even larger, in complexes formed by the concave side of the bowls. These variations can be expected to be related to the sigma-hole value of the halogen, which becomes more positive as its size increases. This effect should be responsible for the changes in the interaction of AT and BT structures, with the σ-hole pointing towards the bowl. However, the intensity of the interaction also increases in BP structures, associated with an increase in dispersion due to the larger size of the molecules. The interaction becomes more intense with the concave face than with the convex one despite the latter having a more negative MEP (see Fig. S2). Hence, it is not the electrostatic interaction the one controlling the interaction, but other aspects determine the final stability. In fact, the structures by the concave face are around -2 to -3 kcal

mol^{-1} more stable than by the convex face, and the difference seems to increase with the size of the halogen, especially in BP structures.

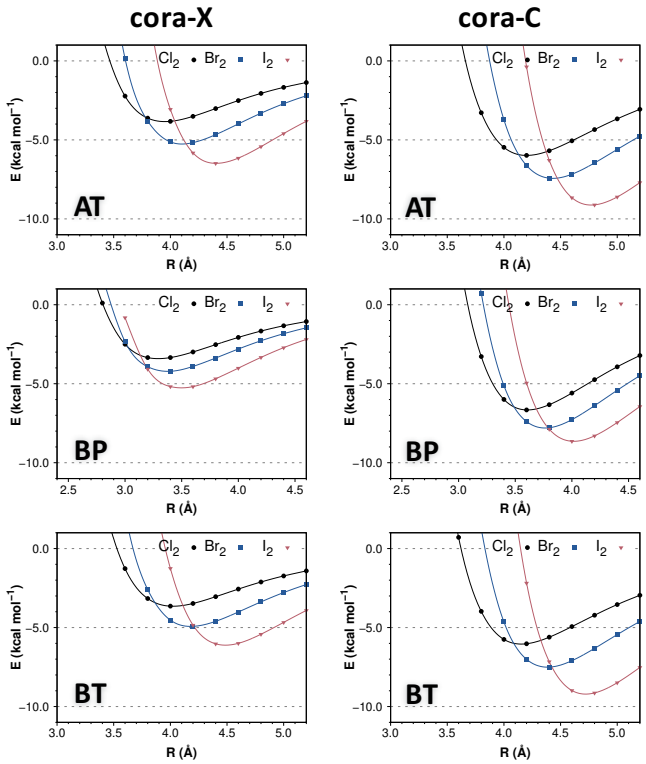

Figure 2. Potential energy curves obtained at the MP2.5 level for the different complexes with corannulene. X and C refer to the convex and concave sides of the bowls, respectively.

Figure 3, showing the energy curves obtained for Br_2 with different aromatic species, helps to compare the behaviour of the different bowls (see Figs. S10 and S11 for Cl_2 and I_2). The first aspect that attracts attention is the differentiated behaviour between the concave and convex faces. In all cases, the complexes with corannulene and sumanene by the convex face are less stable than the complexes with flat coronene. These are relatively small differences, which barely reach 1 kcal mol^{-1} except in BP structures. This behaviour is also observed in chlorine and iodine complexes with similar values. However, the observed behaviour is the opposite by the concave face; in this case all the complexes are more stable than those formed by coronene, and the effect is even greater than by the convex face, reaching variations of -1.5 to -2.0 kcal mol^{-1}.

The observed behaviour clearly shows the effect of curvature on the interaction between halogens and aromatic species. A priori one might expect that in the curved species the electrostatic interaction would be stronger (more negative MEP), but simultaneously the curvature causes the distances between the halogen atoms and the carbon atoms to change with respect to the flat configuration, causing variations in dispersion. Probably, the balance of these two factors determines the trends finally observed. Adding to this effects, there is a

change in equilibrium distances as we go from planar to curved species. All complexes by the concave face show larger distances than analogous dimers with coronene**,** while the opposite is observed by the convex face, leading to shorter equilibrium distances. This is probably related to a decrease on the steric hindrance that allows X_2 to come closer by the convex face of the bowl, because the curvature puts the carbon atoms further away from the X_2 molecule.

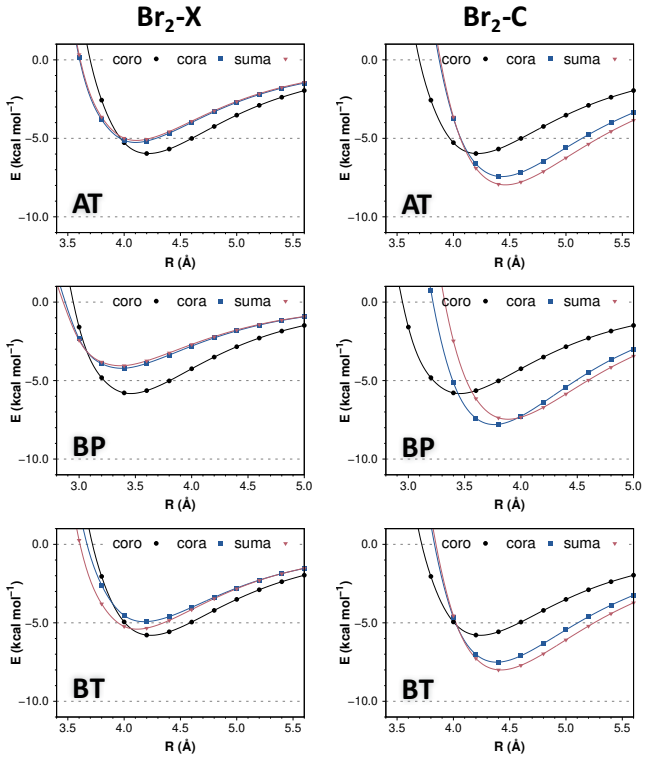

Figure 3. Potential energy curves obtained at the MP2.5 level for the different complexes with Br_2. X and C refer to the convex and concave sides of the bowls, respectively.

3.1.3. SAPT analysis

SAPT0 not only provides appropriate values for the equilibrium distances of the studied complexes as well as reasonable interaction energies. The main characteristic of the SAPT methods is that the interaction energy is not obtained as a difference but by adding contributions to the interaction energy which are physically sound. Depending on the type and number of the contributions, different SAPT levels can be defined.[74, 78] In this work, the SAPT0 model has been used, consisting in contributions to second order using the HF wavefunctions. Despite not including (costly) intramonomer correlation effects, Parker et al. have shown that the combination of SAPT0 with the jun-cc-pVDZ basis set provides good results for a variety of complexes.[74] In fact, the comparison of the values obtained with SAPT0/jun-cc-pVDZ and the MP2.5 reference values is really good. Therefore, SAPT0/jun-cc-pVDZ has been used to obtain potential energy curves as with the rest of the methods, but also to compute the different contributions to the interaction energy. The whole set of SAPT0 results in the minima obtained

by interpolation of the potential energy curves is listed in Supporting Information (Tables S7 and S8).

Overall, the behaviour of all complexes is qualitatively similar. The greatest contribution to the stabilization of the complexes comes from dispersion, that contributes about 60% of the stabilization, followed by the electrostatic contribution that is usually much smaller, contributing around 30%. Therefore, regardless of the type of halogen and its orientation, these complexes are dominated by the dispersive component. Although the overall behaviour is similar, there are differences among the complexes depending on the type of bowl, dihalogen or face by which they interact.

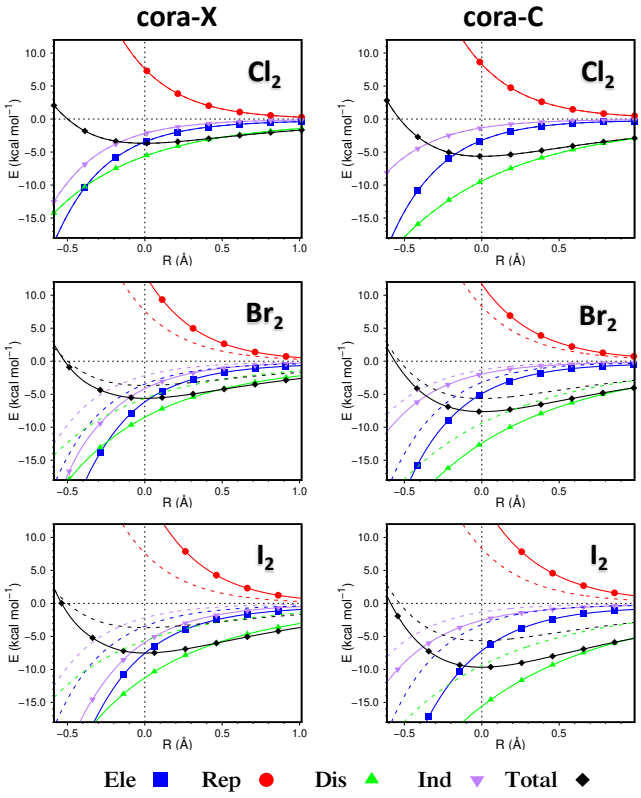

Figure 4. SAPT0 contributions for AT complexes formed by halogens and corannulene. Dotted lines correspond to Cl_2 complexes. Origin at the minima. X and C refer to the convex and concave sides of the bowls, respectively.

The effect of the nature of the halogen on the interaction is shown for AT dimers with corannulene in Figure 4. The origin is at the position of the minima though, as expected, the equilibrium position shifts to longer distances as the halogen size increases. While in the complexes with Br_2 the change is relatively small (around 0.1-0.2 Å larger than Cl_2 complexes) in the complexes with I_2 the equilibrium distances increase by 0.4-0.5 Å. As it can be seen in Figure 4, when switching from Cl_2 to Br_2 to I_2 all contributions to the interaction energy become more intense. There is an increase in repulsion of 5-10 kcal mol^{-1} by the convex face while by the concave face the increase is somewhat smaller (3-7 kcal mol^{-1}). The attractive contribution that

varies the most when changing the halogen is dispersion, which increases with increasing size and always to a larger extent by the concave face. The electrostatic contribution also increases significantly and there is also a significant increase in the induction contribution by the convex face (the larger magnitude of the σ-hole causes larger polarisation as the halogen size increases). This behaviour is already observed in the complexes with coronene (Fig. S12 with AT results for coronene and sumanene; Figs. S13 and S14 for results of BP and BT dimers), being enhanced in the curved systems by the convex face and weakened by the concave one. Thus, as the halogen size increases all contributions to the interaction energy increase resulting in more stable complexes. It is mainly a dispersive effect due to the increase in halogen size, combined with an increase in electrostatic contribution due to the more positive σ-holes.

Figure 5 shows the effect of the Br_2 molecule interacting on either side of the two curved species, corannulene and sumanene (See Figs. S15 and S16 for Cl_2 and I_2). It can be observed that the complexes are always more stable by the concave face than by the convex side, as already commented for the MP2.5 results above, but the final behaviour is the result of a balance between the different contributions to the interaction energy.

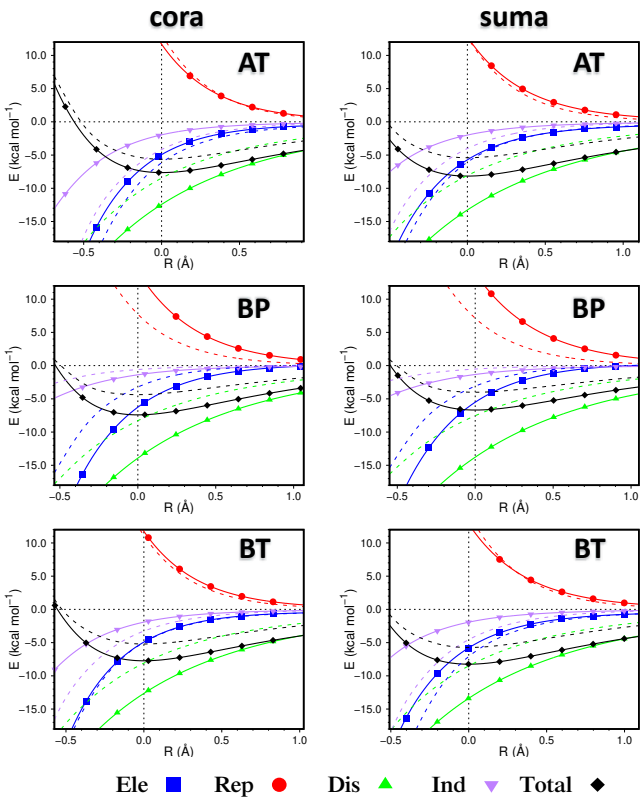

Figure 5. SAPT0 contributions for complexes formed by Br_2 and corannulene and sumanene. Dotted lines correspond to the convex face. Origin at the minima.

Considering the AT complexes, in which the σ-hole is oriented directly towards a carbon atom, it can be observed that there are hardly any changes in the repulsion component, since the halogen can be placed without any steric hindrance from the other atoms of the bowl. The changes in the electrostatic contribution are relatively small and favour the convex face, since the pyramidalisation of the carbon atoms creates a dipole in that direction (in addition, the X_2 molecule can approach more closely). The dominant factor, as expected, is dispersion, which undergoes a significant increase by the concave face, since the curvature of the molecule puts more carbon atoms close to the dihalogens by this face. More surprising is the important contribution of the induction energy, which is usually the least contributing to the stability of neutral complexes. This is a result of the σ-hole directing towards the aromatic surface and polarising the bowl. Induction undergoes a significant decrease when the halogen is located by the concave face, in a similar way as the electrostatic contribution. Therefore, while the concave face is clearly favoured by the increased dispersion, the effect is counterbalanced by the electrostatic and induction terms, which favour the formation of AT complexes by the convex face. The BT complexes have very similar characteristics, since the orientation of the halogen is pretty much the same, only slightly displaced towards the centre of a C-C bond. The case of the BP complexes is different, since the σ-hole is not oriented towards carbon atoms. Although dispersion continues to dominate, the change in the electrostatic component is greater than in the T structures, favouring the concave face. This must be related to the greater proximity between atoms by the concave face producing a greater charge overlap between the halogen and the inner face of the bowl (electrostatic penetration). In BP structures the trends are more complex to analyse since there is a larger steric hindrance by the concave face and the halogen can interact with other regions of the bowl. The repulsion increases significantly by the concave face, as it is the case with dispersion. In this type of complexes, the change in induction is much smaller than in the previous cases, since such an effective polarization cannot be produced. The behaviour described is similar for the rest of the X_2 molecules.

The effect of the bowl on the interaction is represented in Figure 6 for complexes of Br_2 in AT orientation. As a first approximation to the curvature effects on the interaction, the values obtained with corannulene and sumanene are analysed taking coronene as a reference. Overall, there is a clear effect of the face where the halogen interacts, so there is a behaviour clearly differentiated by the concave and the convex face. Thus, the interaction always decreases for complexes with corannulene and sumanene by the convex face compared to similar complexes with coronene, while the opposite is true for the concave face. In Figure 6 the reason for this behaviour can be understood. Considering AT complexes by the convex face (Figs. S17 to 19 for BP and BT), there is a slight increase in repulsion compared to coronene, probably because the equilibrium distance is somewhat shorter. On the other hand, from an electrostatic point of view the curvature favours the interaction, with appreciable increases in both electrostatics and induction. However, the term that determines the final result is the decrease on the contribution of dispersion, which falls in all the complexes and which, together with the increase in repulsion, makes the complexes less stable by the convex face than those formed with coronene. This is due to the fact that the curvature puts the atoms of the bowl further away from the halogen and therefore dispersion decreases. In the case of the complexes by the concave face the effect is the opposite. The repulsion increases, but the curvature puts carbon atoms closer to the halogen molecule and therefore the dispersion increases greatly, being the dominant effect and

the cause that makes the complexes with corannulene and sumanene more stable than with coronene.

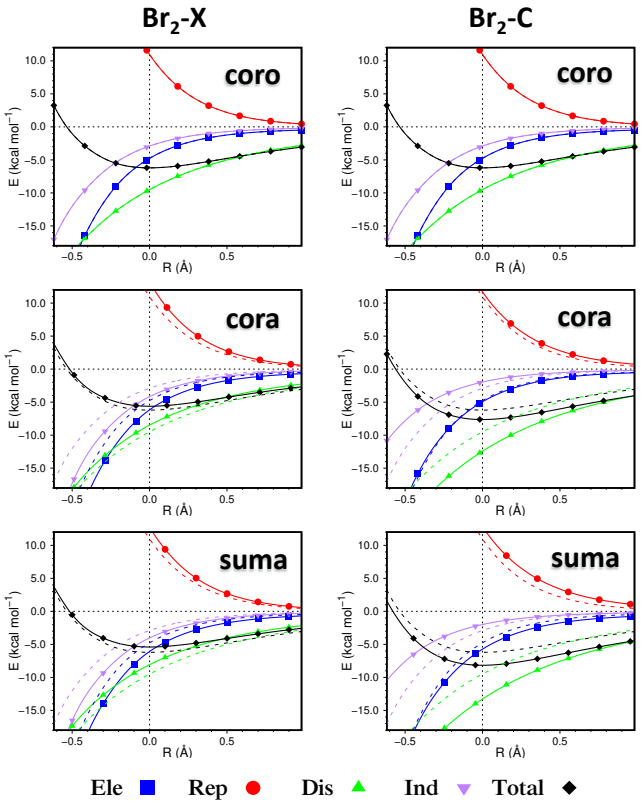

Figure 6. SAPT0 contributions for complexes formed by Br_2 and the different bowls. AT dimers. Dotted lines correspond to coronene complexes. Origin at the minima. X and C refer to the convex and concave sides of the bowls, respectively.

In summary, the curvature causes changes in the different contributions to the interaction energy, but it is a matter of dispersion overall. The concave face is favoured due to a larger dispersion contribution that overcomes the increase in repulsion and the loss of electrostatic and inductive stabilization. Dispersion decreases by the convex side and therefore the complexes are less stable. Thus, compared with a similar planar species, curved aromatic systems form more stable complexes with dihalogens by the concave side, while curving the aromatic surface leads to a loss of stability by the convex face.

3.2. Larger π systems. Complexes with circumcoronene and C_{60}

As already indicated by Kim et al.,[31] coronene complexes are at the limit of undergoing a change on the orientation of the halogen, passing from the most stable T structures with small aromatic systems to the P ones for larger surfaces. It has already been commented above how in coronene complexes the three orientations considered in this work differ in stability by a small amount (0.1-0.3 kcal mol^{-1}), so they can be considered to be practically isoenergetic (Table 1).

To study the effect of employing more extended aromatic systems, complexes of X_2 with circumcoronene and C_{60} have been considered. Circumcoronene complexes allow analysing the effect of enlarging the planar π surface, while C_{60} complexes can be taken as an example of a curved aromatic surface without an edge. Due to the larger size of these species, the calculation of the potential curves with MP2.5 is too expensive. Taking into account the behaviour observed for smaller systems, it has been decided to obtain the potential energy curves with SAPT0/jun-cc-pVDZ and to estimate the interaction energy at the minima at the SCS-MP2/CBS level, which provides results practically identical to the MP2.5 ones for the systems already considered.

Table 2 shows the values obtained for the interaction energy of the complexes formed with circumcoronene. There are no major stability differences, although in all cases the BP structure is favoured. Therefore, as Kim et al. suggested,[31] there is a change in the orientation of the halogen molecule as the size of the aromatic system increases. In any case, the results indicate that the BP structure is favoured for all the halogens considered, and the differences in stability among structures are similar in all cases, so that the T structures are approximately 0.5 kcal mol^{-1} less stable than the BP ones (still, greater differences than in coronene complexes). T structures are stable and could be formed, though they become less favourable compared to P ones as size increases. In the complexes with C_{60} (Table 2) the curvature of the surface is more pronounced than in other systems considered and there is an appreciable decrease on the interaction energy, so that the complexes with C_{60} are the least stable among those considered in this work.

Table 2. Results obtained for complexes with circumcoronene (**circum**) and C_{60}. The equilibrium distance (Å) is obtained with SAPT0. Energies in kcal mol^{-1}.

		AT			BP			BT		
		R	SCS[a]	SAPT0	R	SCS[a]	SAPT0	R	SCS[a]	SAPT0
circum	**Cl_2**	4.03	-5.35	-5.25	3.31	-5.92	-5.85	4.03	-5.30	-5.23
	Br_2	4.18	-7.07	-7.46	3.36	-7.44	-8.07	4.19	-6.99	-7.41
	I_2	4.45	-8.88	-9.81	3.53	-9.54	-10.55	4.46	-8.79	-9.74
C_{60}	**Cl_2**	4.03	-3.18	-3.05	3.31	-3.25	-3.11	4.10	-3.12	-2.93
	Br_2	4.13	-4.43	-4.57	3.33	-4.17	-4.43	4.23	-4.27	-4.28
	I_2	4.40	-5.52	-6.02	3.39	-5.41	-6.00	4.49	-5.35	-5.63

a) SCS indicates SCS-MP2/CBS interaction energies ate the SAPT0 minima.

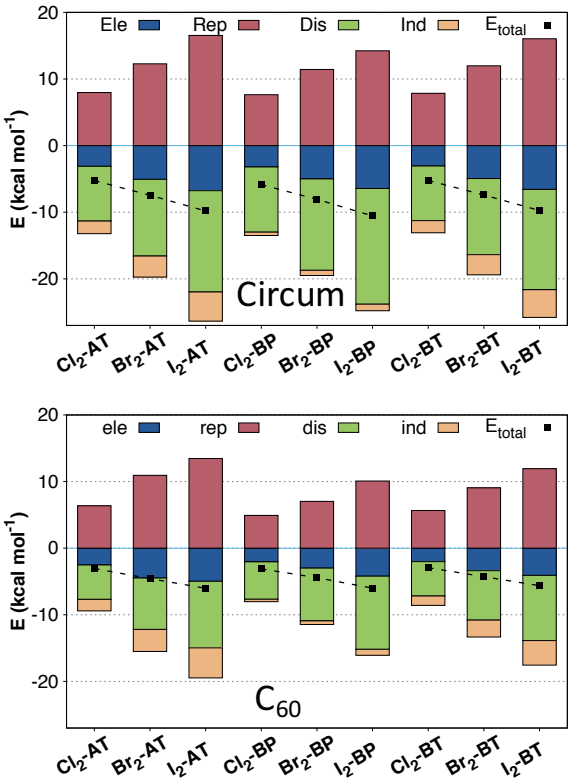

Figure 7. Comparison of the contributions to the interaction energy in larger complexes.

Figure 7 shows the contributions to the interaction energy for these complexes (see values in Table S9). It can be observed that for each structure the stability increases with the size of the halogen in a similar way. In the case of circumcoronene complexes, the increase in stability is associated with increments in all the contributions to the interaction, so that the final balance of attractive contributions overcomes the increase in repulsion and therefore the stability increases. The electrostatic contribution increases significantly with halogen size in the T complexes, but also in the BP ones, with an only slightly smaller magnitude. On the other hand, the variation in the dispersion contribution is the most pronounced one, while induction, as already mentioned above, is only important in T complexes. Comparing among different structures, it is observed that the electrostatic contribution is similar in the three orientations, while repulsion and specially dispersion are more favourable in BP complexes. Only the induction contribution clearly favours the T structures, but to a smaller extent than the combination of repulsion and dispersion in BP ones. In the complexes with C_{60} the situation is similar; electrostatics together with induction favour the T structures, but the effect is practically cancelled out with the changes in repulsion and dispersion, so that the three structures are practically isoenergetic.

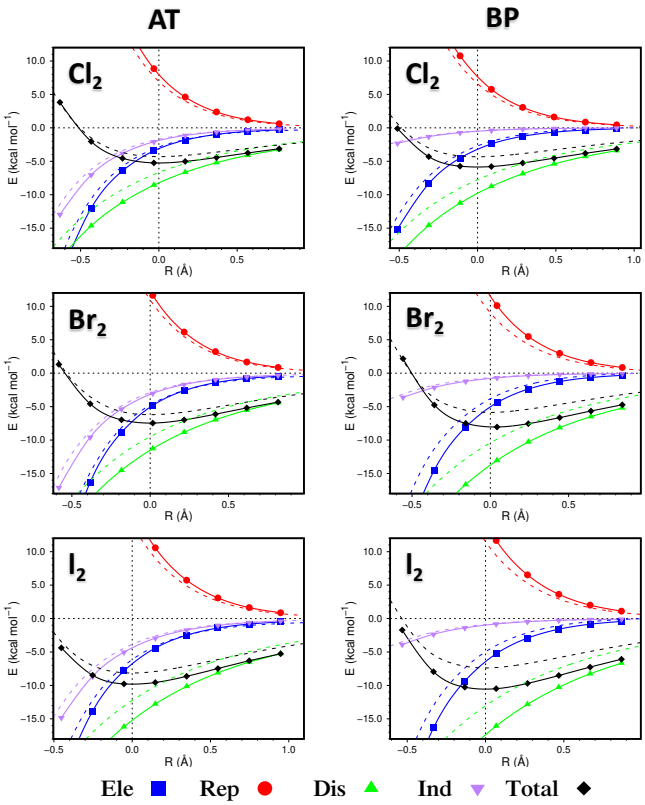

Figure 8. Size effect. Comparison of the contributions to the interaction energy in larger complexes. Circumcoronene complexes (solid lines) vs. coronene ones (dotted lines). The origin corresponds to the equilibrium distance of the circumcoronene complexes.

Comparing the results obtained with circumcoronene with those of coronene (Figure 8, BT in Fig. S20) an estimation of the effect of the extension of the aromatic cloud on the interaction can be obtained. There is a significant increase in electrostatic contribution when going from coronene to circumcoronene, so that the interaction increases by -0.5 kcal mol^{-1} for Cl_2, but already -1.2 kcal mol^{-1} for Br_2 and -1.5 kcal mol^{-1} for I_2. This increase in electrostatic interaction is accompanied by an increase in repulsion, probably due to the shortening of equilibrium distances (0.05-0.08 Å). This increment is larger than that of electrostatics and reaches 1-3 kcal mol^{-1}. However, the most significant change corresponds to dispersion; similarly to π-π interactions[8-11] there seems to be a combined effect of a greater polarizability of the aromatic system that is reflected in greater dispersion as well as a side effect because the repulsive wall softens and allows a decrease in the equilibrium distance. Therefore, going from coronene to circumcoronene an effect associated to the extended size of the aromatic cloud is observed, originating almost exclusively in dispersion. It can be expected that the same trend would be followed in larger similar systems, though caution should be taken in near metallic species, where the behaviour could be different.

Considering the interaction curves without putting the origin at the equilibrium distance (see Fig. S21), it can be clearly observed that the only contribution that varies between coronene and circumcoronene complexes is dispersion. When the change on the position of the minima is considered (the equilibrium distance in circumcoronene complexes is shorter) the differences in

dispersion increase and are accompanied by a greater electrostatic contribution, but this is a consequence of the shorter equilibrium distance and not of the nature of the interacting species.

3.3. Curvature effects in circumcoronene complexes

Finally, the effect of the curvature on the interactions in large aromatic systems has been estimated using circumcoronene as a model. For doing this, circumcoronene has been curved following a cylindrical symmetry (as in a nanotube, Figure 9) using different radii of curvature between 5 and 40 Å. For each radius, the atoms are located accordingly and subsequently optimized at the TPSS-D3BJ/def2-TZVP while keeping all dihedral angles fixed. For each of these curvatures a SAPT0 scan has been made and the minimum of each curve has been determined (set of values in Table S10).

As in planar complexes with circumcoronene, the stacked BP structure is the most stable one in the complexes with the curved system, independently of the X_2 molecule considered. However, the results indicate that, in accordance with those discussed above for corannulene and sumanene complexes, as the curvature increases complexes by the concave face are favoured while those by the convex face are weakened. Since the BP structure is the one that takes more advantage of dispersion, as the curvature increases it undergoes a larger increase in the interaction by the concave face, which gains greater relative stability with respect to the T structures. Similarly, by the convex side the dispersion decays more rapidly in BP structures and, therefore, as the curvature increases the stabilities become closer to those of the AT ones. While for the planar aromatic species the BP structures are around 0.6-0.7 kcal mol^{-1} more stable than the AT ones, in the most curved circumcoronene complexes by the convex face this difference vanishes, so in the case of Br_2 and I_2 AT complexes become slightly more stable. The effect of the curvature by the convex face is relatively small, reaching around 1 kcal mol^{-1} (much larger by the concave side), though capable of tuning the stability of the complexes and even changing their relative stability.

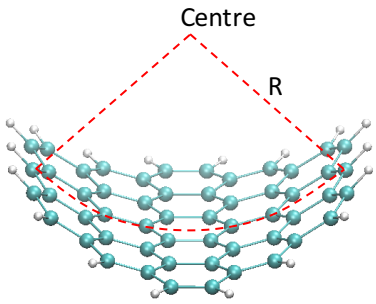

Figure 9. Procedure employed to curve circumcoronene following cylindrical symmetry. R is the radius of the cylinder.

The changes undergone by the complexes as circumcoronene is curved can also be appreciated in Figure 10, showing the changes relative to the planar species (BT complexes in

Fig. S22). As commented above, the stability of the complex decreases by the convex face as the curvature increases, though the changes observed with the curvatures tested are not large and barely reach 1 kcal mol^{-1}. Figure 10 also shows that BP structures are more sensitive to curvature than AT ones. This could be expected for the concave face, since the halogen molecules in BP structures are more effectively surrounded by the curved surface than AT ones; however, BP structures are also more affected by curvature on the convex side.

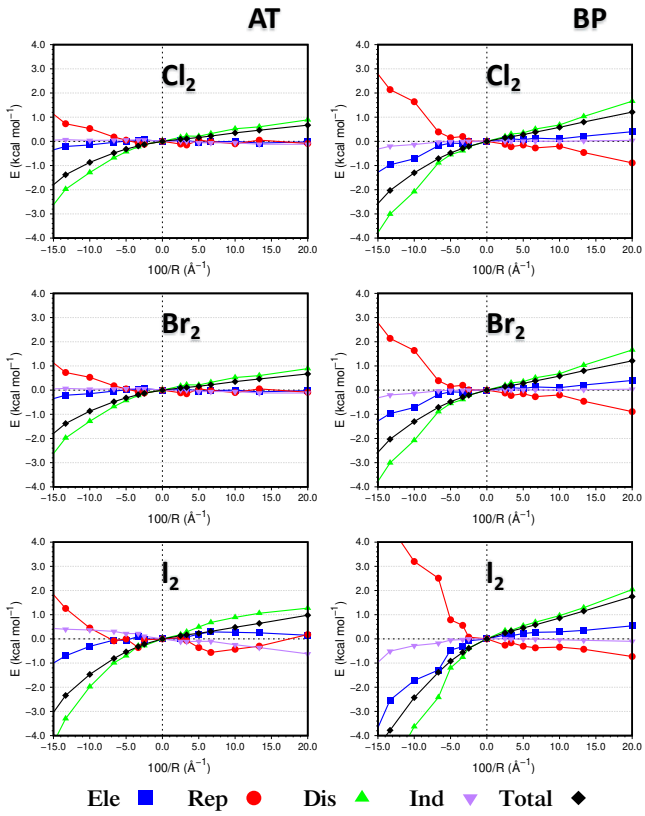

Figure 10. Changes on the interaction energy as the circumcoronene molecule is curved. Negative values correspond to the concave face.

All contributions to the interaction energy change, though induction is almost unaffected except for the largest curvatures. A similar behaviour is observed for electrostatics, so the final stability changes seem to depend on the interplay of dispersion and repulsion. It is worth noticing that electrostatics changes are somewhat larger in BP structures, specially by the concave side, and in fact they seem to be relevant in the stabilization of I_2 complexes as the curvature increases. It can be expected that this increase in electrostatic contribution is related with the larger overlap between the charge distributions of circumcoronene and the halogen. The contributions that change most sharply are repulsion and dispersion, which in some ways are related to the number of nearby atoms.

As the system becomes more curved, repulsion decreases by the convex face, while it increases more rapidly by the concave face due to enhanced steric hindrance. Similarly, the

dispersion contribution decays by the convex face because the carbon atoms move away from the halogens, whereas it raises more rapidly by the concave face due to the closer proximity of the carbon atoms to the dihalogen inside the bowl. Overall, dispersion is the term that dominates the final energy changes and in fact the interaction energy roughly follows the changes on dispersion. However, this behaviour appears to be the consequence of several effects, and electrostatics seems to have a more significant role If the changes are obtained while keeping the intermolecular distances fixed on the value obtained for the planar systems (Fig. S23). When the system is curved, the equilibrium distance slightly changes to larger values by the concave face and to shorter ones by the convex one. Along with these changes in equilibrium distance, the contributions to the interaction energy also change. The changes on electrostatics are decreased, while repulsion changes are surpassed by dispersion ones so the total stability change is mainly controlled by the latter.

4. Conclusions

The intermolecular interaction in complexes formed by the dihalogens Cl_2, Br_2, and I_2 with planar and curved aromatic systems has been studied in order to check the effects of the curvature and extension of the aromatic surface upon the interaction with halogens. The results indicate that the interaction strengthens as the size of the halogen atoms grows, with a larger effect when the dihalogen is located by the concave face of curved systems. In coronene complexes, structures showing a halogen bond (T) are similarly stable as others with the dihalogen stacked onto the aromatic surface (P). T structures are favoured by electrostatics and induction associated to the interaction with the σ-hole, while P dimers take advantage of enhanced dispersion. In complexes with corannulene and sumanene, the balance of these factors results in T structures being more stable by the convex face while P ones are favoured by the concave one. In any case, the most stable complexes are formed when the dihalogen is located by the concave face of curved aromatic species.

The changes on the interaction with curvature are mainly controlled by changes on dispersion despite other possible contributions: by the convex face dispersion decreases relative to planar coronene and the complex is less stable; by the concave face dispersion increases and so it does the stability of the complex. Enlarging the size of the aromatic species favours stacked structures because the presence of a larger number of atoms increases dispersion contributions. A systematic study in complexes with curved circumcoronene confirms that the stability is indeed affected by the curvature of the aromatic surface, with dispersion being the main controlling factor.

Overall, the results indicate that dihalogens do not interact with large aromatic systems by means of halogen bonds, stacked structures being more favourable. Curvature of the aromatic surface favours stacked structures even more when interacting by the concave face, while halogen bonded dimers become relatively favoured by the convex face. However, only for the complexes involving aromatic systems with the largest curvatures tested, halogen bonded dimers become the most stable ones. Thus, it can be expected that except in very curved surfaces as those of small fullerenes or nanotubes, dihalogens will not establish halogen bonds with extended aromatic surfaces but will form stacked dimers.

Acknowledgments

The authors thank the financial support from the Consellería de Cultura, Educación e Ordenación Universitaria e da Consellería de Economía, Emprego e Industria (Axuda para Consolidación e Estruturación de unidades de investigación competitivas do Sistema Universitario de Galicia, Xunta de Galicia ED431C 2017/17). The authors also want to express their gratitude to the CESGA (Centro de Supercomputación de Galicia) for the use of their computers.

Conflicts of interest

There are no conflicts to declare

References

1. E. A. Meyer, R. K. Castellano and F. Diederich, *Angew. Chem. Int. Ed.*, 2003, **42**, 1210-1250.
2. L. M. Salonen, M. Ellermann and F. Diederich, *Angew. Chem. Int. Ed.*, 2011, **50**, 4808-4842.
3. D. W. Johnson and F. Hof, *Aromatic Interactions: Frontiers in Knowledge and Application*, The Royal Society of Chemistry2017.
4. T. Akasaka, A. Osuka, S. Fukuzumi, H. Kandori and Y. Aso, *Chemical Science of π-Electron Systems*, Springer Japan, Tokyo, 2015.
5. N. Martin and J.-F. Nierengarten, *Supramolecular Chemistry of Fullerenes and Carbon Nanotubes*, Wiley-VCH Verlag & Co. KGaA, Weinheim, Germany, 2012.
6. S. Tsuzuki and T. Uchimaru, *Curr. Org. Chem.*, 2006, **10**, 745-762.
7. C. R. Martinez and B. L. Iverson, *Chem. Sci.*, 2012, **3**, 2191-2201.
8. S. Grimme, *Angew. Chem. Int. Ed.*, 2008, **47**, 3430-3434.
9. S. Ehrlich, J. Moellmann and S. Grimme, *Acc. Chem. Res.*, 2013, **46**, 916-926.
10. M. Alonso, T. Woller, F. J. Martín-Martínez, J. Contreras-García, P. Geerlings and F. DeProft, *Chem. Eur. J.*, 2014, 4931-4941.
11. E. M. Cabaleiro-Lago and J. Rodríguez-Otero, *ACS Omega*, 2018, **3**, 9348-9359.
12. A. S. Mahadevi and G. N. Sastry, *Chem. Rev.*, 2013, **113**, 2100-2138.
13. I. Soteras, M. Orozco and F. J. Luque, *Phys. Chem. Chem. Phys.*, 2008, **10**, 2616-2624.
14. A. Frontera, D. Quiñonero and P. M. Deyà, *WIREs Comput. Mol. Sci.*, 2011, **1**, 440-459.
15. B. L. Schottel, H. T. Chifotides and K. R. Dunbar, *Chem. Soc. Rev.*, 2008, **37**, 68-83.
16. M. Nishio, *Phys. Chem. Chem. Phys.*, 2011, **13**, 13873-13900.
17. M. Nishio, Y. Umezawa, J. Fantini, M. S. Weiss and P. Chakrabarti, *Phys. Chem. Chem. Phys.*, 2014, **16**, 12648-12683.
18. G. Cavallo, P. Metrangolo, R. Milani, T. Pilati, A. Priimagi, G. Resnati and G. Terraneo, *Chem. Rev.*, 2016, **116**, 2478-2601.
19. L. C. Gilday, S. W. Robinson, T. A. Barendt, M. J. Langton, B. R. Mullaney and P. D. Beer, *Chem. Rev.*, 2015, **115**, 7118-7195.
20. S. Sirimulla, J. B. Bailey, R. Vegesna and M. Narayan, *J. Chem. Inf. Model., JCIM*, 2013, **53**, 2781-2791.
21. H. Wang, W. Wang and W. J. Jin, *Chem. Rev.*, 2016, **116**, 5072-5104.
22. M. H. Kolář and P. Hobza, *Chem. Rev.*, 2016, **116**, 5155-5187.
23. T. Clark, *Faraday Discuss.*, 2017, **203**, 9-27.
24. P. Politzer, J. S. Murray and T. Clark, *Phys. Chem. Chem. Phys.*, 2013, **15**, 11178-11189.
25. P. Politzer and J. S. Murray, *J. Comput. Chem.*, 2017, 1-8.
26. P. Politzer, J. Murray, T. Clark and G. Resnati, *Phys. Chem. Chem. Phys.*, 2017.
27. A. Forni, S. Pieraccini, S. Rendine and M. Sironi, *J. Comput. Chem.*, 2014, **35**, 386-394.
28. C. Wang, D. Danovich, Y. Mo and S. Shaik, *J. Chem. Theory Comput.*, 2014, **10**, 3726-3737.

29. J. Řezáč and A. de la Lande, *Phys. Chem. Chem. Phys.*, 2017, **19**, 791-803.
30. K. E. Riley, M. Vazquez, C. Umemura, C. Miller and K.-A. Tran, *Chem. Eur. J.*, 2016, **22**, 17690-17695.
31. D. Y. Kim, J. M. L. Madridejos, M. Ha, J.-H. Kim, D. C. Yang, C. Baig and K. S. Kim, *Chem. Commun.*, 2017, **53**, 6140-6143.
32. F. Langa and J.-f. Nierengarten, *Fullerenes: Principles and Applications*, RSC Publishing, Cambridge CB4 0WF, UK, 2012.
33. M. A. Petrukhina and L. A. Scott, *Fragments of fullerenes and carbon nanotubes*, John Wiley & Sons, Inc., Hoboken, New Jersey, 2012.
34. L. T. Scott, H. E. Bronstein, D. V. Preda, R. B. M. Ansems, M. S. Bratcher and S. Hagen, *Pure & Applied Chemistry*, 1999, **71**, 209-219.
35. M. R. Kennedy, L. A. Burns and C. D. Sherrill, *J. Phys. Chem. A*, 2012, **116**, 11920-11926.
36. E. M. Pérez and N. Martín, *Chem. Soc. Rev.*, 2015, **44**, 6425-6433.
37. A. Sygula, F. R. Fronczek, R. Sygula, P. W. Rabideau and M. M. Olmstead, *J. Am. Chem. Soc.*, 2007, **129**, 3842-3843.
38. D. Josa, J. Rodriguez-Otero and E. M. Cabaleiro-Lago, *Phys. Chem. Chem. Phys.*, 2015, **17**, 13206-13214.
39. D. Josa, I. González-Veloso, J. Rodríguez-Otero and E. M. Cabaleiro-Lago, *Phys. Chem. Chem. Phys.*, 2015, **17**, 6233-6241.
40. D. Josa, J. Rodríguez-Otero, E. M. Cabaleiro-Lago, L. A. Santos and T. C. Ramalho, *J. Phys. Chem. A*, 2014, **118**, 9521-9528.
41. D. Josa, L. Azevedo dos Santos, I. González-Veloso, J. Rodríguez-Otero, E. M. Cabaleiro-Lago and T. de Castro Ramalho, *RSC Advances*, 2014, **4**, 29826.
42. P. A. Denis, *RSC Advances*, 2013, **3**, 25296-25305.
43. P. A. Denis, *J. Phys. Org. Chem.*, 2014, **27**, 918-925.
44. P. A. Denis, *New J. Chem.*, 2014, **38**, 5608-5616.
45. T. Kawase and H. Kurata, *Chem. Rev.*, 2006, **106**, 5250-5273.
46. T. Iwamoto, Y. Watanabe, T. Sadahiro, T. Haino and S. Yamago, *Angew. Chem. Int. Ed.*, 2011, **50**, 8342-8344.
47. T. Iwamoto, Y. Watanabe, H. Takaya, T. Haino, N. Yasuda and S. Yamago, *Chem. Eur. J.*, 2013, **19**, 14061-14068.
48. I. González-Veloso, J. Rodríguez-Otero and E. M. Cabaleiro-Lago, *Phys. Chem. Chem. Phys.*, 2016, 31670-31679.
49. I. Gonzalez-Veloso, E. M. Cabaleiro-Lago and J. Rodriguez-Otero, *Phys. Chem. Chem. Phys.*, 2018, **20**, 11347-11358.
50. I. González-Veloso, J. Rodríguez-Otero and E. M. Cabaleiro-Lago, *Struct. Chem.*, 2019, **30**, 647-656.
51. K. Yuan, C.-H. Zhou, Y.-C. Zhu and X. Zhao, *Phys. Chem. Chem. Phys.*, 2015, **17**, 18802-18812.
52. K. Yuan, Y.-J. Guo and X. Zhao, *The Journal of Physical Chemistry C*, 2015, **119**, 5168-5179.
53. E. M. Cabaleiro-Lago, J. Rodríguez-Otero and J. A. Carrazana-García, *Phys. Chem. Chem. Phys.*, 2017, **19**, 26787-26798.
54. J. A. Carrazana-Garcia, J. Rodriguez-Otero and E. M. Cabaleiro-Lago, *J. Phys. Chem. B*, 2011, **115**, 2774-2782.
55. J. A. Carrazana-García, E. M. Cabaleiro-Lago and J. Rodríguez-Otero, *Phys. Chem. Chem. Phys.*, 2017, **19**, 10543-10553.
56. P. Garcia-Novo, A. Campo-Cacharron, E. M. Cabaleiro-Lago and J. Rodriguez-Otero, *Phys. Chem. Chem. Phys.*, 2012, **14**, 104-112.
57. A. Campo-Cacharron, E. M. Cabaleiro-Lago and J. Rodriguez-Otero, *J. Comput. Chem.*, 2014, **35**, 1533-1544.
58. S. Grimme, J. Antony, S. Ehrlich and H. Krieg, *J. Chem. Phys.*, 2010, **132**, 154104.
59. S. Grimme, *WIREs Comput. Mol. Sci.*, 2011, **1**, 211-228.
60. S. Grimme, S. Ehrlich and L. Goerigk, *J. Comput. Chem.*, 2011, **32**, 1456-1465.

61. F. Weigend and R. Ahlrichs, *Phys. Chem. Chem. Phys.*, 2005, **7**, 3297-3305.
62. F. Neese, *WIREs Comput. Mol. Sci.*, 2012, **2**, 73-78.
63. S. F. Boys and F. Bernardi, *Mol. Phys.*, 1970, **19**, 553-566.
64. G. Chalasinski and M. M. Szczesniak, *Chem. Rev.*, 2000, **100**, 4227-4252.
65. E. M. Cabaleiro-Lago, B. Fernández and J. Rodríguez-Otero, *J. Comput. Chem.*, 2018, **39**, 93-104.
66. S. Grimme, L. Goerigk and R. F. Fink, *WIREs Comput. Mol. Sci.*, 2012, **2**, 886-906.
67. S. Grimme, *J. Chem. Phys.*, 2003, **118**, 9095-9102.
68. J. Antony and S. Grimme, *J. Phys. Chem. A*, 2007, **111**, 4862.
69. M. Pitoňák, P. Neogrády, J. Černý, S. Grimme and P. Hobza, *ChemPhysChem*, 2009, **10**, 282-289.
70. R. Sedlak, K. E. Riley, J. Řezáč, M. Pitoňák and P. Hobza, *ChemPhysChem*, 2013, **14**, 698-707.
71. K. E. Riley, J. Rezac and P. Hobza, *Phys. Chem. Chem. Phys.*, 2012, **14**, 13187-13193.
72. K. E. Riley, J. Rezac and P. Hobza, *Phys. Chem. Chem. Phys.*, 2011, **13**, 21121-21125.
73. E. G. Hohenstein and C. D. Sherrill, *WIREs Comput. Mol. Sci.*, 2012, **2**, 304-326.
74. T. M. Parker, L. A. Burns, R. M. Parrish, A. Ryno, G and C. D. Sherrill, *J. Chem. Phys.*, 2014, **140**, 094106.
75. T. Helgaker, W. Klopper, H. Koch and J. Noga, *J. Chem. Phys.*, 1997, **106**, 9639-9646.
76. A. Halkier, T. Helgaker, P. Jørgensen, W. Klopper, H. Koch, J. Olsen and A. K. Wilson, *Chem. Phys. Lett.*, 1998, **286**, 243-252.
77. B. Jeziorski, R. Moszynski and K. Szalewicz, *Chem. Rev.*, 1994, **94**, 1887-1930.
78. K. Patkowski, *WIREs Comput. Mol. Sci.*, 2019, **10**, e1452.
79. F. Weigend, *Phys. Chem. Chem. Phys.*, 2006, **8**, 1057-1065.
80. F. Neese, F. Wennmohs, A. Hansen and U. Becker, *Chem. Phys.*, 2009, **356**, 98-109.
81. R. Izsak and F. Neese, *J. Chem. Phys.*, 2011, **135**, 144105.
82. "Psi4 1.1: An Open-Source Electronic Structure Program Emphasizing Automation, Advanced Libraries, and Interoperability", R. M. Parrish, L. A. Burns, D. G. A. Smith, A. C. Simmonett, A. E. DePrince, E. G. Hohenstein, U. Bozkaya, A. Y. Sokolov, R. Di Remigio, R. M. Richard, J. F. Gonthier, A. M. James, H. R. McAlexander, A. Kumar, M. Saitow, X. Wang, B. P. Pritchard, P. Verma, H. F. Schaefer, K. Patkowski, R. A. King, E. F. Valeev, F. A. Evangelista, J. M. Turney, T. D. Crawford and C. D. Sherrill, *J. Chem. Theory Comput.*, 2017, **13**, 3185-3197.
83. B. P. Pritchard, D. Altarawy, B. Didier, T. D. Gibson and T. L. Windus, *J. Chem. Inf. Model., JCIM*, 2019, **59**, 4814-4820.
84. K. L. Schuchardt, B. T. Didier, T. Elsethagen, L. Sun, V. Gurumoorthi, J. Chase, J. Li and T. L. Windus, *J. Chem. Inf. Model., JCIM*, 2007, **47**, 1045-1052.
85. C. Hättig, G. Schmitz and J. Koßmann, *Phys. Chem. Chem. Phys.*, 2012, **14**, 6549-6555.

TOC

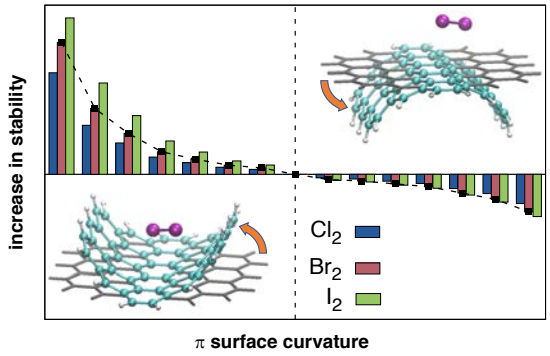

Curvature of aromatic systems strengthens the interaction by the concave face while it weakens by the convex one. Parallel structures are favoured over halogen bonded ones.